Journal of
Synchrotron
Radiation

ISSN 0909-0495

Received 18 October 2012
Accepted 18 March 2013

Impaired pulmonary blood flow distribution in congestive heart failure assessed using synchrotron radiation microangiography

Mikiyasu Shirai,[a] Matthew Beard,[b] James T. Pearson,[c,d] Takashi Sonobe,[a] Hirotsugu Tsuchimochi,[a] Yutaka Fujii,[a] Emily Gray,[b] Keiji Umetani[e] and Daryl O. Schwenke[b]*

[a]Department of Cardiac Physiology, National Cerebral and Cardiovascular Center Research Institute, Suita, Osaka, Japan, [b]Department of Physiology, University of Otago, Dunedin, New Zealand, [c]Department of Physiology and Monash Biomedical Imaging Facility, Monash University, Melbourne, Australia, [d]Australian Synchrotron, Melbourne, Australia, and [e]Japan Synchrotron Radiation Research Institute, Hyogo, Japan. E-mail: daryl.schwenke@otago.ac.nz

Synchrotron radiation microangiography is a powerful tool for assessing adverse changes in pulmonary vessel density associated with primary pulmonary hypertension (PH). Congestive heart failure (CHF) leads to a 'secondary' onset of PH, yet it is unknown whether secondary PH is also associated with reduced vessel density. This study utilized synchrotron radiation to assess both pulmonary vessel density and endothelial function in a Dahl rat model of CHF with secondary PH. High salt-fed Dahl salt-sensitive (Dahl-S) and salt-resistant (Dahl-R) rats were anesthetized and microangiography was performed to assess the pulmonary vessel density and vascular responses to (i) sodium nitroprusside (5.0 $\mu g\ kg^{-1}\ min^{-1}$), (ii) acetylcholine (3.0 $\mu g\ kg^{-1}\ min^{-1}$) and (iii) ET-1_A receptor blockade, BQ-123 (1 $mg\ kg^{-1}$). Dahl-S rats developed CHF and secondary PH as evident by endothelial dysfunction, impaired vasodilatory responses to acetylcholine, enhanced vasodilatory responses to BQ-123 and extensive pulmonary vascular remodeling. Consequently, the pulmonary vessel density was adversely reduced. Interestingly, the etiology of secondary PH manifests with structural and functional changes that are comparable with that previously reported for primary PH. One important discrepancy, however, is that ET-1 modulation of pulmonary vessels is most striking in vessels with a diameter range of 100–200 μm in secondary PH, in contrast to a range of 200–300 μm in primary PH. Such discrepancies should be considered in future studies investigating primary and secondary forms of PH.

Keywords: microangiography; secondary pulmonary hypertension; nitric oxide; endothelin-1.

1. Introduction

Pulmonary hypertension (PH) is an adverse complication typically associated with several lung pathologies, and has a bleak long-term prognosis. For the majority of cases, the onset of PH originates within the lung and is characterized by endothelial and smooth muscle cell proliferation (Sakao *et al.*, 2009), sustained pulmonary vasoconstriction (Oka *et al.*, 2008), vascular smooth muscle remodeling (Guilluy *et al.*, 2009) and vessel rarefaction (Fried & Reid, 1984), all of which contribute to a sustained increase in pulmonary arterial pressure.

PH can also develop secondary to various forms of cardiac diseases, such as congestive heart failure (CHF). Indeed, 60–80% of all patients with CHF will subsequently develop secondary PH (Kerem *et al.*, 2010; Lam *et al.*, 2009). Yet there is a paucity of studies that have examined the etiology for this specific form of PH. The onset of PH, secondary to CHF, is not only due to the 'passive' congestion from venous pooling within the pulmonary vasculature, but also comprises a 'reactive' component, thought to be endothelial dysfunction, that further exacerbates the development of PH (Kerem *et al.*, 2010; Dai *et al.*, 2004; Deuchar *et al.*, 2002).

The endothelium plays a critical role in modulating normal pulmonary vascular tone by releasing various vasoactive mediators, of which endothelin-1 (ET-1), a potent vasoconstrictor (Yuan & Rubin, 2005; Imamura *et al.*, 2005), and nitric oxide (NO), a primary vasodilator (Fike *et al.*, 1998; Le Cras

& McMurtry, 2001), have been identified as major vasomediators. Over the last decade it has become apparent that pulmonary endothelial dysfunction, which impairs the vasoactive pathways for ET-1 and NO, acts as a fundamental trigger in primary PH for instigating structural and functional changes within the pulmonary circulation that, ultimately, impairs blood flow distribution throughout the lung and, hence, increases pulmonary vascular resistance.

Although endothelial dysfunction has been implicated as a possible pathogenic contributor in PH secondary to CHF (Kerem *et al.*, 2010; Moraes *et al.*, 2000), its impact on pulmonary blood flow distribution throughout the lung has not been examined. Moreover, adverse changes in blood flow distribution, if any, may well differ from other primary forms of PH owing to high pulmonary blood flow and 'passive' venous congestion associated with an elevated left ventricular filling pressure in CHF (Yamaki *et al.*, 1997; Dai *et al.*, 2004). Importantly, it is these changes in blood flow distribution that are responsible for the adverse increase in vascular resistance. Ultimately, any discrepancies in the pathological alterations of pulmonary blood flow between primary and secondary forms of PH may impact on the type, and effectiveness, of potential therapeutic interventions (Raoul *et al.*, 2007).

We have previously demonstrated the validity and accuracy of synchrotron radiation (SR) microangiography as an effective tool for assessing changes in the distribution of pulmonary blood vessels, in a closed-chest rat model, associated with two different etiologies of primary PH: chronic hypoxia and monocrotaline (Schwenke *et al.*, 2009). Importantly, the resolution capabilities of SR enable the size of pulmonary vessels with an internal diameter greater than 80 µm, which encompasses the majority of vessels that are adversely affected in PH, to be accurately measured, *in vivo*.

In this study we utilized SR and aimed to assess the extent of pulmonary endothelial dysfunction in a CHF model of PH (using Dahl salt-sensitive rats). Pulmonary vascular and endothelial integrity were assessed by the vasodilatory responses to acetylcholine, exogenous NO and ET-1_A inhibition (BQ-123). Ultimately, however, we aimed to determine whether endothelial dysfunction adversely impairs pulmonary blood flow distribution in secondary forms of PH.

2. Materials and methods

2.1. Ethical approval

All experiments were approved by the local Animal Ethics Committee of SPring-8, and conducted in accordance with the guidelines of the Physiological Society of Japan.

2.2. Animals

Experiments were conducted on 14 male Dahl rats (14 weeks old; body weight $\simeq$ 290–350 g); Group 1: Dahl salt-sensitive rats (Dahl-S; $n = 7$); Group 2: Dahl salt-resistant rats (Dahl-R; $n = 7$). The two groups of Dahl rats were fed a high-salt diet consisting of 8% NaCl pellets for eight weeks, prior to angiography experiments. For comparative purposes, data previously obtained from 'normal' Sprague Dawley (SD) rats (*i.e.* no high-salt diet) in an earlier study (Schwenke *et al.*, 2011) are also presented (Group 3: SD; $n = 7$). All rats were on a 12 h light/dark cycle at 278 $\pm$ 1 K and provided with food and water *ad libitum*. Dahl-S rats developed CHF due to the severe and sustained systemic hypertension, as a result of the high-salt diet (see section 3).

2.3. Anesthesia and surgical preparation

On the day of the angiography experiment, each rat was anesthetized with Nembutal sodium (pentobarbital sodium) using an induction dose of 60 mg kg^{-1} (i.p.) followed by a secondary dose of 30 mg kg^{-1} (i.p.). Subsequently, supplementary doses of anesthetic were periodically administered ($\sim$15 mg kg^{-1} h^{-1} i.p.) to maintain a surgical level of anesthesia, evident by the complete absence of the limb withdrawal reflex. Throughout the experimental protocol body temperature was maintained at 310 K using a rectal thermistor coupled with a thermostatically controlled heating pad. Prior to surgery, the skin regions to be cut were infiltrated with intradermal injections ($\sim$0.5 ml) of 1% xylocaine (lidocaine) to ensure local analgesia. The trachea was cannulated and the lungs ventilated with a rodent ventilator (SN-480-7; Shinano, Tokyo, Japan). A femoral artery and vein were cannulated for measurement of systemic arterial blood pressure (ABP) and drug administration, respectively. A 20-gauge BD Angiocath catheter (Becton Dickinson, Utah, USA), with the tip at a 30° angle, was inserted into the jugular vein and advanced into the right ventricle for administering contrast agent as well as intermittently measuring right ventricular pressure (RVP).

2.4. SR microangiography

The pulmonary circulation of the anesthetized rat was visualized using SR microangiography at the BL28B2 beamline of the SPring-8 facility, Hyogo, Japan. We have previously described in detail the accuracy and validity of SR for visualizing the pulmonary microcirculation in a closed-chest rat (Schwenke *et al.*, 2007). The rat was securely fastened to a clear perspex surgical plate, which was then fixed in a vertical position in front of the beam pathway, so that the SR beam would pass perpendicular to the sagittal plane from anterior to posterior through the upper segment of the left lobe (*i.e.* between the second and third rib) and ultimately to a SATICON X-ray camera. Although the effects of gravity might be expected to cause regional heterogeneity in vascular responsiveness, preliminary experiments confirmed that the segment of the lung selected for imaging best represented the pulmonary circulation as a whole in terms of anatomical layout and vascular responsiveness.

2.5. Experimental protocol

Once the rat was in position, heart rate and ABP data were continuously recorded. RVP was also continuously recorded, except during vessel imaging, when the three-way stopcock on the right ventricle catheter was opened to a clinical autoinjector (Nemoto Kyorindo, Tokyo, Japan), which was used to

inject a single bolus of contrast agent (Iomeron 350; Eisai, Tokyo, Japan) at high-speed (0.4 ml at 0.4 ml s^{-1}). For each 2 s period of scanning (a single exposure sequence), 100 frames were recorded. Rats were given at least 10 min to recover from each bolus injection of contrast agent.

Following baseline imaging, rats were administered (i.v.): (i) the NO donor sodium nitroprusside, an endothelium-independent vasodilator (SNP, 5.0 μg kg^{-1} min^{-1} for 5 min), (ii) acetylcholine, an endothelium-dependent vasodilator (ACh, 3.0 μg kg^{-1} min^{-1} for 5 min) and (iii) BQ-123, an ET_A receptor antagonist (1 mg kg^{-1}).

Lung microangiography was performed after the fifth minute of infusing ACh or SNP, and 10 min after BQ-123 administration. Rats had at least 20 min to recover between each drug/test. The doses of all pharmacological agents used in this study are based on well documented recommendations in the literature as well as our own previous reports (Schwenke *et al.*, 2011).

2.6. Morphometric analysis

Following the completion of each experiment, rats were euthanized *via* anesthetic overdose (pentobarbital sodium) and the heart excised. The atria were removed and the right ventricle wall separated from the left ventricle and septum. Tissues were blotted and weighed and normalized to 100 g body weight. Right and left ventricular weights were expressed as the ratio of the RV to the left ventricle + septum weight ($W_{RV}/W_{LV+septum}$, Fulton's ratio).

Sections of the left lung and left ventricle were fixed in 4% paraformaldehyde, and subsequently embedded in paraffin. Cross sections, 10 μm thick, were stained with hematoxylin and eosin for examination by light microscopy. Left ventricular wall-thickness and lumen size were measured along four different diameter planes and the average value presented. In addition, the wall-to-lumen ratio of the pulmonary arteries was measured in 34 muscular arteries (ranging in size from 150 to 400 μm in external diameter) as previously described (Schwenke *et al.*, 2011).

2.7. Immunofluorescence

The following antibodies were purchased as indicated: mouse monoclonal to ET-1 (ab2786, Abcam) and rabbit polyclonal to eNOS (ab66127, Abcam). After fixation with 10% formalin (Sigma-Aldrich Ref. HT50-1-2) and embedding in paraffin, 5 μm sections were deparaffinized, rehydrated and antigen retrieval was performed on samples for eNOS analysis using a citric acid buffer. Antibody detection was achieved using Alexa Fluor 488 goat anti-mouse (A-11001, Invitrogen) and Alexa Fluor 568 goat anti-rabbit (A-11011, Invitrogen) antibodies for ET-1 and eNOS, respectively.

2.8. Data acquisition and analysis

The RVP and ABP signals were detected using separate Deltran pressure transducers (Utah Medical Products, Utah, USA), the signals were relayed to Powerlab bridge amplifiers (ML117, AD Instruments Pty, Japan Inc.), and then continuously sampled at 500 Hz with an eight-channel MacLab/8s interface hardware system (AD Instruments), and recorded on a Macintosh Power Book G4 using *Chart* (version 7.0, AD Instruments). Heart rate was derived from the arterial systolic peaks.

All imaged vessel branches were counted. Vessels were categorized according to internal diameter (ID): 100–200 μm, 200–300 μm and 300–500 μm. The ID of 104 vessels, comprising four branching generations, was measured in seven Dahl-S rats, and the ID of 70 vessels was measured in seven Dahl-R rats. The ID of 94 vessels was measured in seven SD rats. The ID of individual vessels was measured under basal conditions and then in response to each of the experimental conditions.

2.9. Image analysis.

The computer-imaging program *Image Pro-plus* (version 4.1, Media Cybernetics, Maryland, USA) was used to enhance contrast and the clarity of angiogram images [see Schwenke *et al.* (2009) for a full description]. The line-profile function of *Image Pro-Plus* was used as an accurate method for measuring the ID of individual vessels (Schwenke *et al.*, 2009). A 50 μm-thick tungsten filament, which had been placed directly across the corner of the detector's window, appeared in all recorded images and was subsequently used as a reference for calculating vessel ID (μm), assuming negligible magnification.

2.10. Statistical analysis

All statistical analyses were conducted using *Statview* (version 5.01, SAS Institute, North Carolina, USA). All results are presented as mean ± standard error of the mean (s.e.m.), except for the number of vessel branches for each of the branching generations, which are presented as mean ± standard deviation (s.d.). One-way ANOVA was used to test for (i) significant differences in vessel caliber under basal conditions compared with each of the experimental conditions (*e.g.* ACh, SNP, BQ-123) and (ii) differences between Dahl-S and Dahl-R rats, as well as values previously recorded for SD rats. Where statistical significance was reached, *post hoc* analyses were incorporated using the paired, or unpaired, *t*-test with Dunnet's correction for multiple comparisons. A P-value $\leq$ 0.05 was predetermined as the level of significance for all statistical analysis.

3. Results

3.1. Hemodynamic and morphometric analysis

A high-salt diet caused severe systemic hypertension in Dahl-S rats (MABP = 194 ± 10) and mild, but still significant, hypertension was evident in Dahl-R rats (MABP 149 ± 4 mmHg). However, only Dahl-S rats exhibited evidence of chronic heart failure, such as ventricular wall thinning and an increase in heart weight (Fig. 1), especially left ventricular mass (indicative of cardiac remodeling; Table 1). As a result, Dahl-S rats developed mild pulmonary hypertension (sRVP = 33.9 mmHg; Table 1), resulting in significant medial thickening

Table 1
Heart weight (*a*) and baseline hemodynamic (*b*) data from Dahl salt-resistant rats (n = 7) and Dahl salt-sensitive rats (n = 7).

Both groups of Dahl rats were fed a high-salt diet (8% NaCl) for eight weeks prior to experimentation and tissue retrieval. For comparative purposes, data are also presented for Sprague Dawley (SD) rats, which were obtained from an earlier study (2011). Data are presented as mean ± s.e.m.

(*a*)	Dahl-R	Dahl-S	SD
Heart weight/100 g body weight (mg)	295 ± 6	375 ± 3†‡	284 ± 10
RV/100 g (mg)	65 ± 5	77 ± 4.7†§	65 ± 4
LV + Septum /100 g (mg)	230 ± 3.9	298 ± 3.8†§	219 ± 9
RV/LV + Septum	0.28 ± 0.02	0.26 ± 0.02	0.30 ± 0.02
Pulmonary vascular wall thickness, lumen ratio	0.266 ± 0.018	0.635 ± 0.078†‡	0.254 ± 0.008

(*b*)	Dahl-R	Dahl-S	SD
sRVP (mmHg)	25.0 ± 1.5	33.9 ± 1.5†§	29.0 ± 0.9
MABP (mmHg)	147.7 ± 4.3§	194.3 ± 10.4†‡	123 ± 7
HR (min^{-1})	346.9 ± 40.9	290.2 ± 51§	395 ± 22

† Significant difference between Dahl-S and Dahl-R (P < 0.01). ‡ Significantly different from SD values (P < 0.01). § Significantly different from SD values (P < 0.05).

of medium-sized pulmonary arteries (150 µm to 400 µm) and an increase in the vascular wall thickness-to-lumen diameter ratio (Table 1), and, ultimately, significant right ventricular hypertrophy (Table 1). The magnitudes of right and left ventricular hypertrophy were comparable, hence Fulton's ratio remained unchanged (RV/LV + Sep ratio of ∼0.26; Table 1).

3.2. SR microangiography

The pulmonary vascular remodeling and increase in pulmonary arterial pressure in Dahl-S rats were well correlated with a reduction in pulmonary vessel density throughout the pulmonary circulation, which was assessed using SR microangiography. The baseline angiograms presented in Fig. 2(*a*) highlight the difference in the pulmonary branching patterns for Dahl-S rats, compared with Dahl-R (and SD) rats, ranging from the axial artery to the fourth-generation of branching. The total number of vessel branches visible within each baseline image (*i.e.* 9.5 mm × 9.5 mm imaging window) was quantified in the same region and field of view for all animals. Importantly, Dahl-S rats had an impaired pulmonary blood flow distribution, evident by a significant reduction in the number of perfused (radiopaque) vessels, primarily of the fourth branching generation (24 ± 2 vessels), compared with Dahl-R rats (31 ± 2) and SD rats (30 ± 2) (Fig. 2*b*).

3.3. Immunofluorescence of eNOS and ET-1

Immunofluorescence staining was performed to 'qualitatively' assess the localization and expression of ET-1 and eNOS protein in the pulmonary vessels of the left lung of Dahl-S and Dahl-R rats (*cf.* SD rats). As illustrated in Fig. 3, positive-staining (fluorescence) for both ET-1 and eNOS, localized primarily within the endothelium, appear elevated in Dahl-S rats 'relative' to both Dahl-R and SD rats.

3.4. Endothelium-independent vasodilation: responses to sodium nitroprusside

Exogenous NO (SNP at 5 µg kg^{-1} min^{-1} for 5 min) caused significant pulmonary vasodilation of similar magnitude for all groups of rats, evident by an increase in the ID of vessels <300 µm (for Dahl-S rats) and/or <200 µm (for Dahl-R and SD rats) (Fig. 4). In spite of the obvious vasodilation, the corresponding decrease in sRVP (*e.g.* 14% decrease in sRVP for SD rats) did not reach statistical significance for any of the groups of rats (Fig. 5). SNP did not alter heart rate (HR) but it did significantly reduce systemic ABP in all rats (Fig. 5).

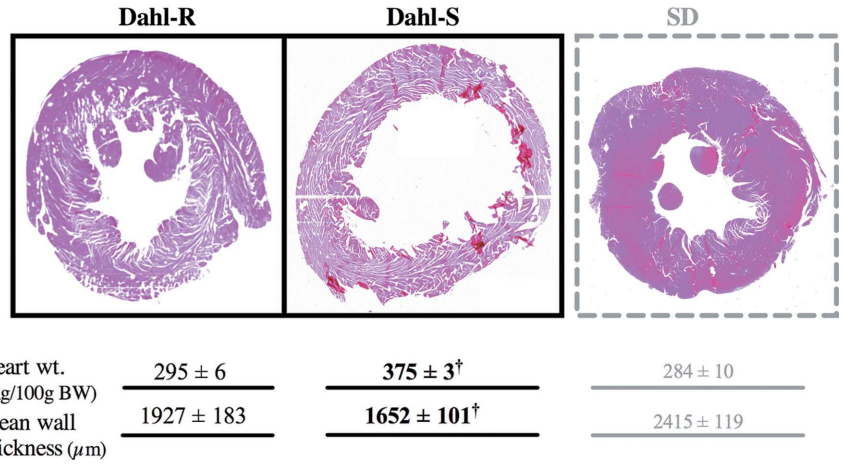

Figure 1
(*a*) Histology photomicrographs of sections of the left ventricle retrieved Dahl salt-resistant (Dahl-R) and salt-sensitive (Dahl-S) rats and Sprague Dawley (SD) rats. (*b*) Quantitative analysis of heart weight (per 100 g body weight) and left ventricle wall thickness for each of the three groups of rats. Data are presented as mean ± s.d. †Significant difference between Dahl-S and Dahl-R rats (P < 0.05).

3.5. Endothelium-dependent vasodilation: responses to acetylcholine

ACh (3.0 µg kg^{-1} min^{-1} for 5 min, i.v.) causes pulmonary vasodilation in SD rats, most notably in the 100–200 µm vessels (20% increase in ID; Fig. 4*c*), which is associated with a 14% decrease in sRVP (Fig. 5) (Schwenke *et al.*, 2011). Importantly the magnitude of vasodilation in response to ACh (% increase in vessel ID) was comparable with that observed for SNP (Fig. 4*c*), indicating uncompromised endothelial function.

Similarly, in Dahl-R rats the significant magnitude of ACh-induced vasodilation (100–300 µm vessels) was also comparable with that of SNP (Fig. 4*b*). In Dahl-S rats, however, the ACh-induced vasodilation was significantly attenuated, particularly of the 100–

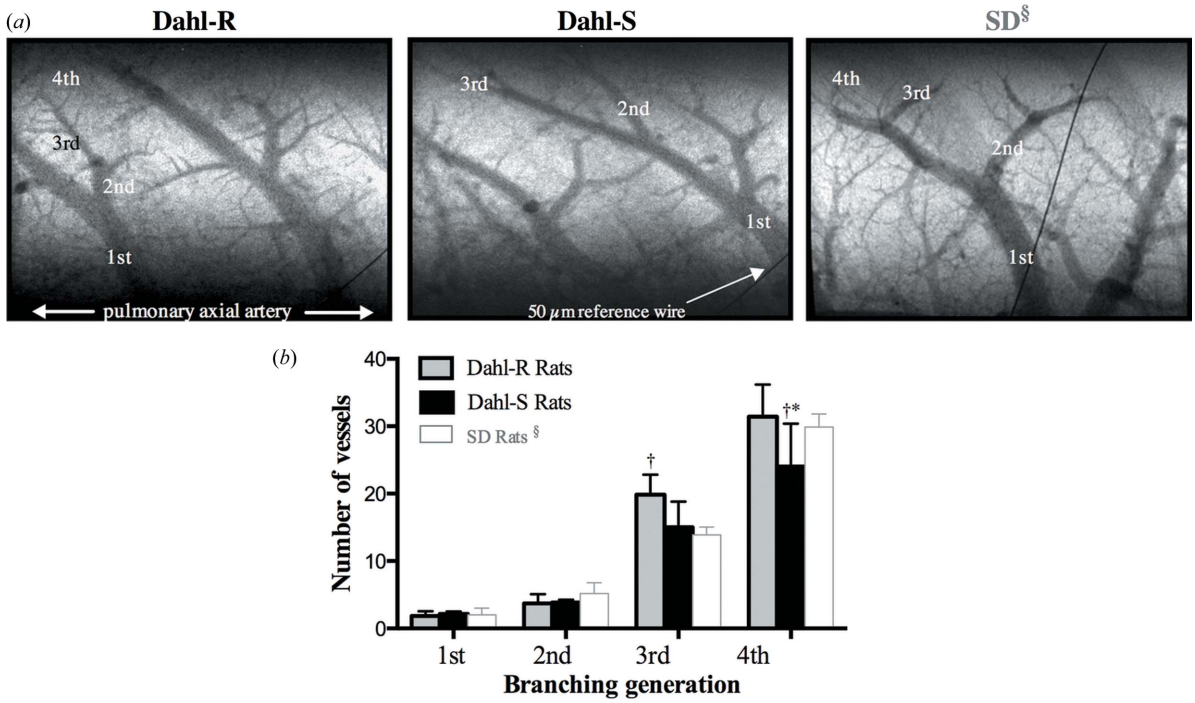

Figure 2
(*a*) Microangiogram images showing the baseline branching pattern (to the fourth generation) of small pulmonary arteries, and (*b*) the number of opaque vessels (mean ± s.e.m.) at each of the first four branching generations of the pulmonary circulation in Dahl salt-resistant rats (Dahl-R; $n = 7$) and salt-sensitive rats with secondary PH (Dahl-S; $n = 7$). Data are also provided for SD rats for comparative purposes [§ taken from Schwenke *et al.* (2011)]. The tungsten wire in each angiogram image is a reference of diameter 50 µm. *Significant difference between Dahl-R and Dahl-S rats ($P < 0.05$). †Significantly different from SD rats ($P < 0.05$).

200 µm vessels (11% increase in ID) compared with that observed for SNP (21% increase in ID) (Fig. 4*a*), reflecting significant endothelial dysfunction. Interestingly, despite the significant dilatation, ACh did not significantly decrease sRVP in Dahl-R or Dahl-S rats (Fig. 5). ACh significantly reduced systemic ABP in all rats, but did not alter HR.

3.6. Inhibition of endothelin-1_A receptor (BQ-123)

ET-1_A receptor blockade (BQ-123, 1 mg kg^{-1}) caused considerable vasodilation of the small microvessels in Dahl-S rats (22% increase in ID of the 100–200 µm vessels), which was significantly greater than that of Dahl-R rats (Fig. 4*d*). Interestingly, BQ-123 did not significantly dilate any of the pulmonary vessels in Dahl-R rats. Despite the dynamic changes in vessel caliber, ET-1_A receptor blockade did not significantly change sRVP in any of the groups of rats (Fig. 5). BQ-123 caused a small, albeit significant, 10% reduction in MABP in Dahl-S rats only. HR was not altered by BQ-123 in any of the groups of rats (Fig. 5).

4. Discussion

The primary findings of this study show that the development of CHF in Dahl salt-sensitive rats was accompanied by (i) the development of secondary PH and pulmonary vascular remodeling and (ii) impaired endothelium-dependent vasodilation and an enhanced vasodilatory response to ET-1_A

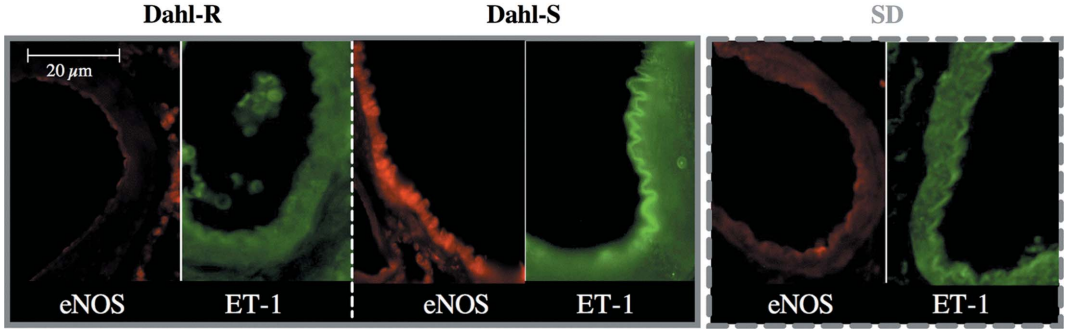

Figure 3
Qualitative assessment of immunofluorescent images highlighting the localized expression of ET-1 (green) and eNOS (red) within the pulmonary endothelium of Dahl salt-resistant (Dahl-R) and salt-sensitive (Dahl-S) rats, as well as SD rats (for comparative purposes). Protein expression (fluorescence) within the pulmonary endothelium 'appears' elevated in Dahl-S rats (ET-1 and eNOS) compared with Dahl-R rats and SD rats.

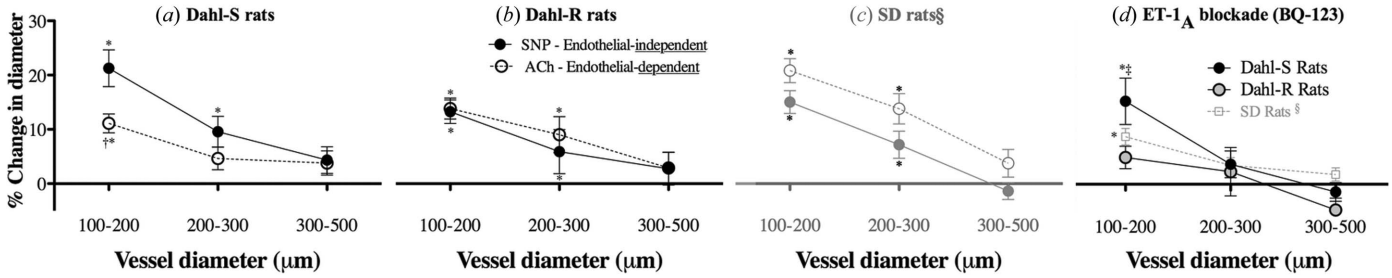

Figure 4
The relationship between vessel size and the magnitude of pulmonary vasomotor responses (% change in vessel internal diameter) in (*a*) Dahl salt-sensitive rats (Dahl-S; $n = 7$), (*b*) Dahl salt-resistant rats (Dahl-R; $n = 7$) and, for comparative purposes, (*c*) SD rats [§taken from Schwenke *et al.* (2011)] in response to the i.v. administration of sodium nitroprusside (SNP, 5.0 μg kg^{-1} min^{-1} for 5 min; closed circles) and ACh (3.0 μg kg^{-1} min^{-1} for 5 min; open circles). (*d*) Magnitude of vasomotor response of all groups of rats in response to ET-1$_A$ receptor blockade (BQ-123, 1 mg kg^{-1}). *Significant reduction/increase in vessel caliber ($P < 0.05$). †Significant difference in the magnitude of response to ACh *versus* SNP ($P < 0.05$). ‡Significant difference between Dahl-R and Dahl-S rats ($P < 0.05$).

receptor blockade. Collectively, these structural and function changes within the pulmonary vasculature ultimately impaired pulmonary blood flow distribution in Dahl-S rats.

According to the World Health Organization, '*Cardiovascular diseases are the number one cause of death globally: more people die annually from CVDs than from any other cause*' (WHO, 2005). CHF is associated with an increase in left ventricular filling pressure, which results in a 'passive' increase in pulmonary venous pressure. Subsequently, a 'reactive' dysfunction of the pulmonary vascular endothelium is thought to further exacerbate the increase in pulmonary vascular resistance (Kerem *et al.*, 2010; Lam *et al.*, 2009).

By utilizing the high-resolution capabilities of SR microangiography, we have consistently shown that pulmonary blood flow distribution is impaired in distinctly different forms of 'primary' PH, evident by a significant reduction in the number of perfused vessels (third to fourth branching generation), within a closed-chest rat model (Schwenke *et al.*, 2009). Similarly, in this study pulmonary blood flow distribution was impaired in Dahl salt-sensitive rats with PH 'secondary' to CHF, which appears comparable with other primary forms of PH that we have investigated. The observation that varying etiologies of PH all similarly impair blood flow distribution raises the question of whether primary and secondary forms of PH share a common 'trigger' for instigating the adverse structural (*e.g.* vascular remodeling) and functional (*e.g.* reduced vasodilatory capacity) changes within the pulmonary vasculature.

Although the pathomechanisms governing PH remain to be fully elucidated, dysfunction of the pulmonary endothelium plays a critical role in the cascade of events that ultimately culminate in the development of not only primary forms of PH (Budhiraja *et al.*, 2004; Sakao *et al.*, 2009) but also PH secondary to CHF (Deuchar *et al.*, 2002; Dai *et al.*, 2004; Kerem *et al.*, 2010; Moraes *et al.*, 2000). In this study we observed that endothelium-dependent vasodilation was impaired in rats with CHF-induced secondary PH, which is consistent with other reports in the literature (Deuchar *et al.*, 2002; Kerem *et al.*, 2010). Moreover, using the novel technology of SR microangiography, we were able to show for the first time that the small microvessels (ID $\simeq$ 100–200 μm) were most susceptible to impairment of endothelium-mediated vasodilation.

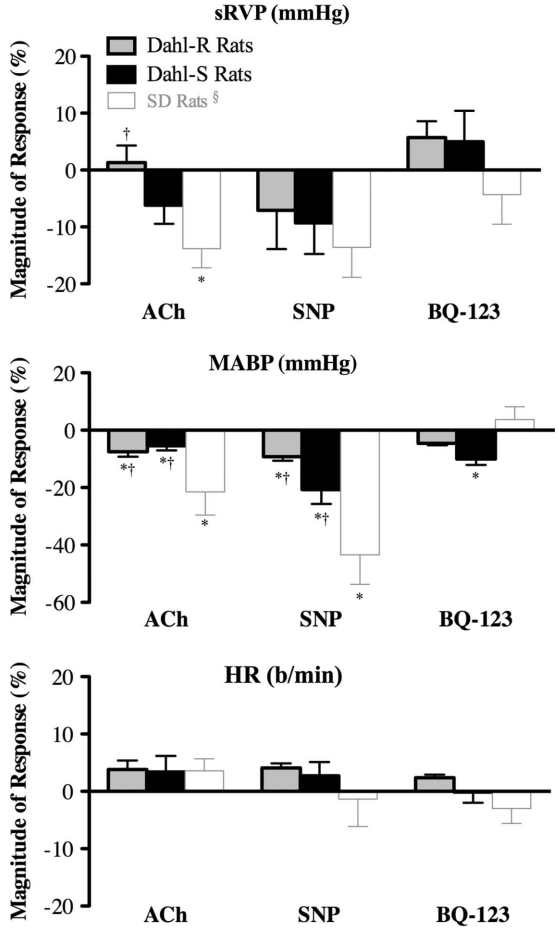

Figure 5
Transient changes (% change) in systolic right ventricular pressure (sRVP), mean arterial blood pressure (MABP) and heart rate (HR) in response to (*a*) ACh (3.0 μg kg^{-1} min^{-1} for 5 min), (*b*) sodium nitroprusside (SNP, 5.0 μg kg^{-1} min^{-1} for 5 min) and (*c*) BQ-123 (1 mg kg^{-1}) for Dahl salt-resistant rats (Dahl-R; $n = 7$) and salt-sensitive rats (Dahl-S; $n = 7$). For comparative purposes, data for SD rats are also presented [§taken from Schwenke *et al.* (2011)]. *Significant increase/decrease in response to each intervention ($P < 0.05$). †Significantly different to SD rats ($P < 0.05$).

The impaired vasodilatory capacity is unlikely due to a decrease in the expression of eNOS, since both immunofluorescence (this study) and quantitative Western blot analysis (Dai *et al.*, 2004; Kerem *et al.*, 2010) indicate that eNOS, localized within the pulmonary endothelium, is elevated in CHF rats. Rather, the diminished endothelium-dependent vasodilation may be due to impaired endothelial intracellular calcium signaling (Kerem *et al.*, 2010) and/or a reduction in NO bioavailability (Murata *et al.*, 2001; Raoul *et al.*, 2007) due to an increase in NO degradation (Passauer *et al.*, 2005; Mathew *et al.*, 2002). Despite the impaired endothelium-mediated vasodilation reported in this study, the sensitivity of the vascular smooth muscle to exogenous NO (SNP) was not compromised in Dahl CHF rats with PH, which concurs with that observed in a rat model with primary PH (Schwenke *et al.*, 2011).

We further showed in this study that Dahl CHF rats with secondary PH had an accentuated pulmonary vasodilatory response to the ET-1_A antagonist, BQ-123. Moreover, immunofluorescence suggests that endogenous ET-1 protein levels appear elevated in CHF rats. Indeed, the ET-1 vasoactive pathway is up-regulated, not only in primary forms of PH (Yang *et al.*, 2000; Blumberg *et al.*, 2002) but also in PH secondary to CHF (Dai *et al.*, 2004; Deuchar *et al.*, 2002; Moraes *et al.*, 2000). These results and previous reports may suggest that the 'reactive' pathological change in ET-1 modulation of the pulmonary circulation is similar for both primary and secondary PH. However, at least one significant discrepancy exists.

In primary PH, the small pulmonary arteries and mid-sized arterioles (ID $\simeq$ 200–300 µm) are most susceptible to enhanced sensitivity to exogenous ET-1 (vasoconstriction) and endogenous BQ-123 (Schwenke *et al.*, 2011). In this study, however, the sensitivity of the 200–300 µm vessels to BQ-123 was not adversely altered (*i.e.* similar for all groups of rats). Rather, it was the smaller microvessels (ID $\simeq$ 100–200 µm) that were most susceptible to the adverse increase in sensitivity to BQ-123. Although the reason for this apparent discrepancy is unclear, it should be noted that the initial onset of PH secondary to CHF results from pulmonary venous congestion causing a retrograde increase in pulmonary pressure (Moraes *et al.*, 2000). Consequently, the gradual onset of PH is likely to adversely impact on the smaller arterioles (ID $\simeq$ 100–200 µm) before the larger resistant vessels (ID $\simeq$ 200–300 µm), as commonly observed in primary PH.

Studies that have investigated the pathogenesis of PH secondary to CHF have utilized varying models of heart failure such as acute coronary artery ligation (Deuchar *et al.*, 2002; Jasmin *et al.*, 2003) or aortic banding (Dai *et al.*, 2004; Kerem *et al.*, 2010). In this study we used the Dahl salt-sensitive rat CHF model as a clinically relevant model of one of the fastest growing cardiovascular contributors to CHF, *i.e.* systemic hypertension. Moreover, Klotz *et al.* (2006) recently described the Dahl rat as 'an excellent model to study the pathogenesis of heart failure in the setting of hypertension'. However, as highlighted above, the use of a high-salt diet to induce CHF in Dahl rats can directly impair the endothelial function and, thus, must be taken into consideration when interpreting the effects of CHF on the pathogenesis of PH.

In summary, the development of PH secondary to CHF is caused by 'passive' pulmonary venous congestion, which is likely exacerbated by 'reactive' dysfunction of the pulmonary vascular endothelium. Moreover, although endothelial dysfunction is consistently evident in both primary and secondary PH, adverse changes in ET-1 modulation of pulmonary vessels is most striking in the vessels with a diameter range of 100–200 µm in secondary PH, in contrast to a range of 200–300 µm in primary PH. The underlying mechanisms remain unclear and, accordingly, warrant further research to identify potential targets for therapeutic strategies, especially considering that up to 80% of all patients with CHF will subsequently develop secondary PH.

The work was supported, in part, by the Department of Physiology (University of Otago), a University of Otago Research Grant, an Otago Medical Research Foundation Grant (AG293), a Grant-in-Aid for Scientific Research (20590242) from the Ministry of Education, Culture, Sports, Science and Technology of Japan, a Health and Labour Sciences Research Grants (Research on Intractable Diseases, No. H22-Nanti-ippan-033). The authors are extremely grateful for the technical assistance provided by Ms Isabel Campillo and Ms Carol Bussey. The synchrotron radiation experiments were performed at BL28B2 at SPring-8 with the approval of the Japan Synchrotron Radiation Research Institute (proposal No. 2009B1328).

References

Blumberg, F. C., Lorenz, C., Wolf, K., Sandner, P., Riegger, G. A. & Pfeifer, M. (2002). *Cardiovasc. Res.* **55**, 171–177.
Budhiraja, R., Tuder, R. M. & Hassoun, P. M. (2004). *Circulation*, **109**, 159–165.
Dai, Z. K., Tan, M. S., Chai, C. Y., Yeh, J. L., Chou, S. H., Chiu, C. C., Jeng, A. Y., Chen, I. J. & Wu, J. R. (2004). *Pediatr. Pulmonol.* **37**, 249–256.
Deuchar, G. A., Docherty, A., MacLean, M. R. & Hicks, M. N. (2002). *Br. J. Pharmacol.* **135**, 1060–1068.
Fike, C. D., Kaplowitz, M. R., Thomas, C. J. & Nelin, L. D. (1998). *Am. J. Physiol.* **274**, L517–L526.
Fried, R. & Reid, L. M. (1984). *J. Appl. Physiol.* **57**, 1247–1253.
Guilluy, C., Eddahibi, S., Agard, C., Guignabert, C., Izikki, M., Tu, L., Savale, L., Humbert, M., Fadel, E., Adnot, S., Loirand, G. & Pacaud, P. (2009). *Am. J. Respir. Crit. Care Med.* **179**, 1151–1158.
Imamura, M., Luo, B., Limbird, J., Vitello, A., Oka, M., Ivy, D. D., McMurtry, I. F., Garat, C. V., Fallon, M. B. & Carter, E. P. (2005). *J. Appl. Physiol.* **98**, 739–747.
Jasmin, J. F., Calderone, A., Leung, T. K., Villeneuve, L. & Dupuis, J. (2003). *Cardiovasc. Res.* **58**, 621–631.
Kerem, A., Yin, J., Kaestle, S. M., Hoffmann, J., Schoene, A. M., Singh, B., Kuppe, H., Borst, M. M. & Kuebler, W. M. (2010). *Circ. Res.* **106**, 1103–1116.
Klotz, S., Hay, I., Zhang, G., Maurer, M., Wang, J. & Burkhoff, D. (2006). *Hypertension*, **47**, 901–911.
Lam, C. S., Roger, V. L., Rodeheffer, R. J., Borlaug, B. A., Enders, F. T. & Redfield, M. M. (2009). *J. Am. Collect. Cardiol.* **53**, 1119–1126.
Le Cras, T. D. & McMurtry, I. F. (2001). *Am. J. Physiol.* **280**, L575–L582.

Mathew, R., Yuan, N., Rosenfeld, L., Gewitz, M. H. & Kumar, A. (2002). *Heart Dis.* **4**, 152–158.
Moraes, D. L., Colucci, W. S. & Givertz, M. M. (2000). *Circulation*, **102**, 1718–1723.
Murata, T., Yamawaki, H., Hori, M., Sato, K., Ozaki, H. & Karaki, H. (2001). *Eur. J. Pharmacol.* **421**, 45–53.
Oka, M., Fagan, K. A., Jones, P. L. & McMurtry, I. F. (2008). *Br. J. Pharmacol.* **155**, 444–454.
Passauer, J., Pistrosch, F., Büssemaker, E., Lässig, G., Herbrig, K. & Gross, P. (2005). *J. Am. Soc. Nephrol.* **16**, 959–965.
Raoul, W., Wagner-Ballon, O., Saber, G., Hulin, A., Marcos, E., Giraudier, S., Vainchenker, W., Adnot, S., Eddahibi, S. & Maitre, B. (2007). *Respir. Res.* **8**, 8.
Sakao, S., Tatsumi, K. & Voelkel, N. F. (2009). *Respir. Res.* **10**, 95.
Schwenke, D. O., Pearson, J. T., Shimochi, A., Kangawa, K., Tsuchimochi, H., Umetani, K., Shirai, M. & Cragg, P. A. (2009). *J. Hyperten.* **27**, 1410–1419.
Schwenke, D. O., Pearson, J. T., Sonobe, T., Ishibashi-Ueda, H., Shimouchi, A., Kangawa, K., Umetani, K. & Shirai, M. (2011). *J. Appl. Physiol.* **110**, 901–908.
Schwenke, D. O., Pearson, J. T., Umetani, K., Kangawa, K. & Shirai, M. (2007). *J. Appl. Physiol.* **102**, 787–793.
WHO (2005). *Preventing Chronic Diseases; a Vital Investment.* WHO Global Report. Geneva: World Health Organization.
Yamaki, S., Endo, M. & Takahashi, T. (1997). *Tohoku J. Exp. Med.* **182**, 83–91.
Yang, X., Chen, W. & Li, F. (2000). *Hua Xi Yi Ke Da Xue Xue Bao*, **31**, 30–33.
Yuan, J. X. & Rubin, L. J. (2005). *Circulation*, **111**, 534–538.